www.sciencemag.org/cgi/content/full/319/5871/1805/DC1

Supporting Online Material for

Sr Lattice Clock at 1×10^{-16} Fractional Uncertainty by Remote Optical Evaluation with a Ca Clock

A. D. Ludlow, T. Zelevinsky, G. K. Campbell, S. Blatt, M. M. Boyd,
M. H. G. de Miranda, M. J. Martin, J. W. Thomsen, S. M. Foreman, Jun Ye,*
T. M. Fortier, J. E. Stalnaker, S. A. Diddams, Y. Le Coq, Z. W. Barber,
N. Poli, N. D. Lemke, K. M. Beck, C. W. Oates

*To whom correspondence should be addressed. E-mail: ye@jila.colorado,edu

Published 28 March 2008, *Science* **319**, 1805 (2008)
DOI: 10.1126/science.1153341

This PDF file includes:

SOM Text
Fig. S1
References

Supporting Online Material –

Sr lattice clock at 1x10^{-16} fractional uncertainty by remote optical evaluation with a Ca clock

A. D. Ludlow, T. Zelevinsky, G. K. Campbell, S. Blatt, M. M. Boyd, M. H. G. de Miranda, M. J. Martin, J. W. Thomsen, S. M. Foreman, and Jun Ye

JILA, National Institute of Standards and Technology and University of Colorado, Department of Physics, University of Colorado, Boulder, CO 80309-0440, USA

T. M. Fortier, J. E. Stalnaker, S. A. Diddams, Y. Le Coq, Z. W. Barber, N. Poli, N. D. Lemke, K. M. Beck, and C. W. Oates

National Institute of Standards and Technology, 325 Broadway, Boulder, CO 80305, USA

Supporting documentation is provided for our manuscript Ref. [1].

I. ADDITIONAL EXPERIMENTAL DETAILS

To prepare the atomic sample for the Sr clock, we use narrow-line Doppler cooling techniques to reach μK temperatures. Approximately 4000 ^{87}Sr atoms at 2.5 μK are confined in a 1-D optical standing wave generated by retroreflecting an incident laser with intensity I_0. The resulting longitudinal (transverse) trap frequency is 42 kHz (120 Hz). The lattice trap depth corresponds to 35 times the lattice photon recoil energy. The atom density ρ_0 is approximately $1x10^{11}$ cm^{-3}. Further experimental details can be found elsewhere (*23,9*). Although both clock states have electronic angular momentum J=0, the nuclear spin I=9/2 permits ten spin states, all of which are populated in the ground clock state after laser cooling. We optically pump the lattice-trapped ground state population to the $m_F = \pm 9/2$ states by exciting the $^1S_0$ F=9/2 - $^3P_1$ F'=7/2 transition. The efficacy of this optical pumping is shown in Fig. 1B, where spectroscopy of the π clock transitions is shown with and without optical pumping.

After clock spectroscopy, atomic population remaining in $^1S_0$ is measured by collecting $^1S_0$-$^1P_1$ fluorescence (see Fig. 2A). This nearly resonant excitation lasts a sufficiently long time to both measure the $^1S_0$ atom number and heat this population out of the trap. To measure the $^3P_0$ population, we then optically pump the $^3P_0$ population to $^3S_1$, where decay to $^1S_0$ occurs through $^3P_1$ and we again collect $^1S_0$-$^1P_1$ fluorescence. We combine these measurements to yield a normalized excitation fraction insensitive to number fluctuations of atoms loaded into the lattice. Due to occupation of a variety of longitudinal and transverse motional states, atoms in the 1-D lattice experience different Rabi frequencies from clock excitation (*8*). Inhomogeneities such as this one limit our total excitation fraction to ~80%. After probing the π-transition for $m_F = 9/2$, we re-load a new atom sample and probe the π-transition for $m_F = -9/2$. We stabilize the clock laser to these two transitions by time multiplexing two independent servos, and the digital average of the two line centers serves as the atomic reference.

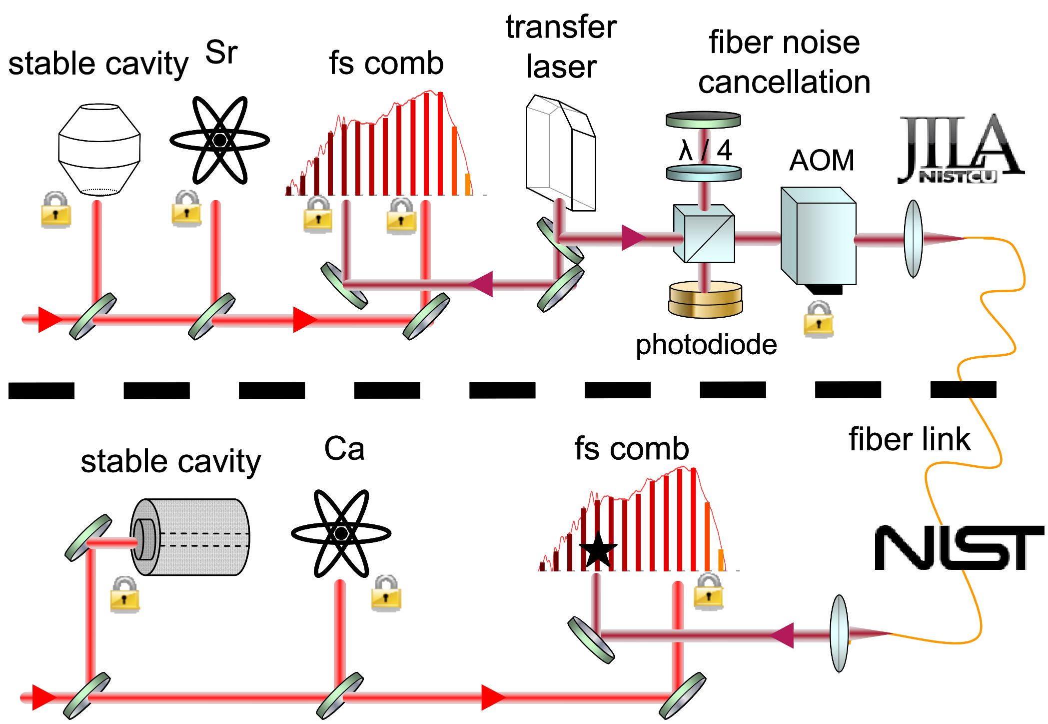

Figure S1

Further details on the experimental setup implemented for comparing the Sr clock to the Ca clock are shown in Figure S1. Each phase lock is pictorially represented by a pad lock. The optical local oscillator for the Sr clock is a diode laser pre-stabilized to a highly-stable, high-finesse optical cavity. The frequency of this pre-stabilized light is then locked to the Sr clock transition with a low-bandwidth servo that controls a frequency shifter between the cavity and the atomic sample. The JILA frequency comb is phase-locked to the Sr clock laser, and the Nd:YAG laser for fiber transfer is in turn phase-locked to the JILA frequency comb. The accumulated phase noise over the fiber connecting JILA and NIST is eliminated by stabilizing the round trip phase of the 1064 nm Nd:YAG light to a local copy. Strictly speaking, the Nd:YAG light received at NIST is syntonized (with exactly the same frequency, but a constant phase offset), but not synchronized, with the local light at JILA. At NIST, the NIST frequency comb is locked to the Ca clock laser, which itself is a diode laser at 657 nm pre-stabilized to a high-finesse cavity and further locked to the Ca clock transition. The measurement (location denoted by the star) is made by comparing a tooth of the NIST comb (stabilized to Ca) against the transferred Nd:YAG light (which is phase-stabilized to Sr). The techniques used to phase-lock the frequency combs and employ them in comparisons between optical standards have been verified to have a 1 s instability of 2 x 10^{-17} and residual uncertainty of near 1 x 10^{-19} [2, 3, 4, 5].

II. ADDITIONAL DETAILS FOR SYSTEMATIC UNCERTAINTIES

Here we provide additional details of the evaluation of systematic uncertainties of the Sr optical clock summarized in Table 1 of Ref. [1].

The two clock states have different polarizabilities at the clock transition frequency. Consequently, the clock probe laser introduces a minute AC Stark shift. The small detuning of the probe laser from couplings to other motional states can lead to such shifts, but this effect is much smaller than coupling to other electronic states. Imperfect alignment between the probe and the lattice axes leads to degradation in the transverse Lamb-Dicke condition and necessitates an increased probe power to excite the clock transition. By strongly saturating the transition with excess probe intensity, we measure a non-zero shift, which is consistent with the known dynamic polarizabilities at 698 nm. By scaling to the intensity value typically used for clock operation, the shift is found to be

$2(1)\times10^{-17}$. More careful probe alignment, interrogation in a 3-D lattice, and longer probe times can further decrease the required probe power and the resulting shift.

Quantum confinement in the well-resolved-sideband limit means that Doppler effects are manifested in the sideband structure which can be isolated from the clock transition. These effects are further suppressed in the Lamb-Dicke regime where photon recoil is transferred to the optical potential. However, off-resonant, weakly excited motional transitions can pull the center frequency of the clock transition. More relevant is line-pulling originating from transitions of other spin states with residual populations after imperfect atomic polarization (typically <5%). Fortunately, many such effects largely occur in a symmetric fashion such that the line-pulling, already small, is reduced. Furthermore, the 20 μT bias *B*-field separates excitation of neighboring spin states by more than two linewidths. The overall line-pulling effect is conservatively estimated to be $<2\times10^{-17}$. We also note that the second-order Doppler effect is suppressed to much below 1×10^{-18}, taking into account atomic motions inside the lattice and residual motions of the lattice potential with respect to the probe beam.

Servo errors in steering the clock laser to the atomic transition can also result in frequency offsets. Our digital servo operates via standard modulation techniques by probing the half maxima of the resonance. Noise processes around the modulation frequency, round-off error, and asymmetric probe laser power spectrum are potential contributors to the servo error. In our system, we are mostly concerned with residual laser drifts and finite loop gain. We typically implement a linear feed-forward frequency compensation for drift of the stable cavity to which the clock laser is locked. This feed-forward value is estimated by measuring the laser drift relative to a Cs-calibrated hydrogen maser through the frequency comb. To overcome imperfect feed-forward compensation, we utilize two integration stages in the laser-atom feedback loop. Operating properly, this approach keeps residual drifts compensated by the primary servo integrator to a measured value of <1 mHz/s. From analysis of the overall servo signal record we conservatively estimate the servo error to be $<5 \times 10^{-17}$.

To improve estimation of the blackbody radiation-induced shift, the differential static polarizabilty of the clock states can be measured with a variety of approaches. One technique is to measure the static polarizability directly by observing a clock shift as a well-controlled DC electric field is applied to the atoms [6]. Another is to constrain the static polarizability value with knowledge of the dynamic polarizability. Unfortunately, at least five dipole couplings contribute to the $^3P_0$ BBR shift above the 1% level, complicating an accurate extrapolation of the dynamic polarizability to DC. Measuring the dynamic polarizability with lasers at BBR wavelengths could be effective, especially if nearby well-known atomic transitions can be used to self-calibrate the optical field strength. Finally, as discussed in the main text, one approach we propose is to cool and trap the atoms in a standard chamber, and then transport them in a moving lattice to a secondary chamber, which has a much more well-defined blackbody environment. At the highest clock accuracy level, it is important to account for the effect of the transmissivity of glass viewports for visible and infrared wavelengths on the blackbody environment. The small chamber needs accurate temperature control at the 10 mK level and would require the use of only small, far-removed optical access to introduce the optical lattice and probe beams. The effective blackbody emissivity of the interior can reach nearly unity and the total BBR environment can be known at the $1\text{x}10^{-4}$ level, necessary for 10^{-18} clock uncertainty.

References:

[1] A. D. Ludlow *et al*., *Science* **319**, 1805 (2008).

[2] J. E. Stalnaker *et al*., Absolute Optical Frequency Measurement of the Hg^+ Standard with a Fractional Frequency Uncertainty at 1×10^{-15}, Appl. Phys. B **89**, 167 (2007).

[3] L.-S. Ma *et al*., Optical frequency synthesis and comparison with uncertainty at the 10^{-19} level, Science **303**, 1843 (2004).

[4] S. A. Diddams *et al*., An optical clock based on a single trapped $^{199}Hg^+$ ion, Science **293**, 825 (2001).

[5] T. R. Schibli, D. C. Yost, M. J. Martin, J. Ye, I. Hartl, A. Marcinkevičius, and M. E. Fermann, Optical frequency comb with sub-mHz linewidth and >10 W average power, Nature Photonics, in press (2008).

[6] E. Simon, P. Laurent, and A. Clairon, Measurement of the Stark shift of the Cs hyperfine splitting in an atomic fountain, Phys. Rev. A **57**, 436 (1998).